Coupling of a new porphyrin photosensitizer and cobaloxime cocatalyst for highly efficient photocatalytic H_2 evolution

Govardhana Babu Bodedla,[a,b] Wai-Yeung Wong*[b] and Xunjin Zhu*[a]

a. Department of Chemistry and Institute of Advanced Materials, Hong Kong Baptist University, Waterloo Road, Kowloon Tong, Hong Kong, P. R. China. E-mail: xjzhu@hkbu.edu.hk.

b. Department of Applied Biology & Chemical Technology and Research Institute for Smart Energy, The Hong Kong Polytechnic University, Hong Kong, P. R. China; The Hong Kong Polytechnic University Shenzhen Research Institute, Shenzhen 518057, P. R. China. E-mail: wai-yeung.wong@polyu.edu.hk.

Photocatalytic hydrogen evolution (PHE) is a promising strategy to produce environmentally friendly clean energy with the use of solar power and water. For this, developing an efficient and nobel metal free photocatalytic system (PS) comprising of high light-harvesting and photostable photosensitizers is an important and challenging task. Herein, a new porphyrin photosensitizer ZnDC(*p*-NI)PP, containing two naphthalimide (NI) donor chromophores and 4-carboxyphenyl substituents is developed for PHE. Using chloropyridinecobaloxime (CoPyCl) as cocatalyst in phosphate buffer/THF solution at pH 7.4, the homogeneous PS of ZnDC(*p*-NI)PP produces a very high hydrogen evolution rate (ηH_2) of 35.70 mmol g^{-1} h^{-1}, turnover number (TON) of 5958 and apparent quanum efficiency (AQE) of 10.01%. This perfomance recorded under the same conditions is signifiantly higher than the PS of ZnDCPP which lacks the NI moieties (ηH_2 of 4.64 mmol g^{-1} h^{-1}, TON of 1397 and AQE of 1.30%), the typical PS of ZnTCPP with four 4-carboxyphenyl substituents groups (ηH_2 of 2.43 mmol g^{-1} h^{-1}, TON of 562 and AQE of 1.00%), and previously reported ZnD(*p*-NI)PP containing only two NI chromophores (ηH_2 of 3.8 mmol g^{-1} h^{-1}, TON of 590 and AQE of 1.5 %). The noticeable performance of ZnDC(*p*-NI)PP in PHE is attributed to the intramolecular energy transfer from the NI donor chromophore to the porphyrin acceptor that would promote the long-lived photoexcitation states. At the same time, the anionic form ($-COO^-$) of 4-carboxyphenyl substituents at pH 7.4 enables a faster electron transfer from porphyrin to cationic Co(III) potentially due to electrostatic force. To the best our knowledge, the PHE results of ZnDC(*p*-NI)PP represent the best one for porphyrin photosensitizers and coabaloxime PSs reported so far. This work paves a new direction for developing new porphyrin-based materials for efficient PHE through facile molecular structure engineering.

Introduction

Solar light-driven splitting of water into hydrogen as carbon free fuel and environmentally friendly clean energy is a promising strategy for reducing consumption of natural fossil fuel resources and greenhouse effect.[1-4] To produce photocatalytic hydrogen evolution (PHE), the photocatalytic systems (PSs) mainly contain three components such as photosensitizer, sacrificial electron donor and cocatalyst. Based on this multicomponent PS design, Lehn and co-workers first reported decent PHE results using $Ru(bpy)_3^{2+}$ as a photosensitizer, triethanolamine (TEOA) as a sacrificial donor and colloidal Pt as a cocatalyst.[5] After a huge number of multicomponent homogeneous/heterogeneous PSs have been developed by employing different combinations of photosensitizers such as Ru-, Ir- and Re-based complexes (noble metals),[6-8] inorganic composites,[7, 9] porous materials,[10 11] organic small molecules and polymers,[7, 12-14] graphitic carbon nitride (g-C_3N_4) polymeric materials,[15, 16] porphyrin derivatives[17-20] and their hybrids with g-C_3N_4/graphene oxide[21] and cocatalysts such as colloidal Pt,[7, 22] Ni-, Fe- and Co-based complexes[23-27] with the use of sacrificial donors such as triethylamine (TEA), ascorbic acid (AA) and TEOA. Although the PSs comprising either noble metal based photosensitizers or cocatalyst (e.g. Pt) produced highly efficient PHE, they cannot be commercialized in the near future due to the high cost of noble metals. To tackle this

problem, researchers are mainly devoted to use noble metal free photosensitizers and cocatalysts for the preparation of PSs. Among the noble metal free photosensitizers, recently, porphyrin derived materials have attracted enormous interest in the PHE owing to their strong solar light absorbing nature in the maximum UV-Vis region, long-lived photoexcited states and possession of suitable HOMO and LUMO energy levels for efficient photoinduced charge separation and their transfer to cocatalyst.[17, 18, 28]

On the other hand, cobalt complexes, especially, cobaloximes as cocatalyst have received tremendous interest due to their easy synthesis, reasonable photostability and high PHE efficiencies due to low reduction potential.[25, 29] Importantly, understanding of electron transfer between the components of PSs is the main criteria to improve the PHE. For this, preparation of PSs in fully homogeneous condition is required. So development of new PSs comprising of porphyrin photosensitizers and cobaloxime cocatalyst in homogeneous condition for high performance PHE is not only a prerequisite but also a necessary condition to pave this research field towards our modern society. However, though a very few homogeneous PSs featuring porphyrin photosensitizers and cobaloxime cocatalyst for PHE have been reported so far, they are not much efficient and stable due to weak light absorbing nature of porphyrins and their photo instability.[30, 31] Thus, we aimed to develop highly efficient PSs for PHE by enhancing the light absorbing properties and photostability of porphyrin photosensitizers.

We have recently found that the linear substitution of di-naphthalimide (NI) moieties at *meso*-position of porphyrin core greatly improved the light absorption, stability of photoexcited states, photoinduced charge separation and photostability of porphyrin photosensitizers and thus PHE.[32] This could be attributed to the efficient intramolecular energy transfer from the NI donor chromophore to the porphyrin acceptor. In this study, we used heterogeneous conditions to evaluate the PHE of di-NI conjugated porphyrin, ZnD(*p*-NI)PP with the use of Pt cocatalyst. Though the PS of ZnD(*p*-NI)PP delivered efficient PHE results, it is not a cost-effective approach and the intrinsic photocatalytic cyclic mechanism was also not much fully addressed due to the usage of Pt and heterogeneous photocatalytic conditions, respectively. In order to prepare a cost-effective, efficient and homogeneous PSs, herein we have developed a new porphyrin photosensitizer, ZnDC(*p*-NI)PP bearing two NI donor chromophores and two -COOH groups and tested its PHE properties using chloropyridinecobaloxime (CoPyCl) cocatalyst under homogeneous phosphate buffer/THF conditions. We presume that, upon light irradiation on ZnDC(*p*-NI)PP porphyrin, this produces long-lived photoexcited states due to occurrence of energy transfer between NI donor chromophore and porphyrin acceptor resulting from the overlap between the emission profile of NI and absorption of porphyrin moiety. As a result, the ZnDC(*p*-NI)P efficiently accepts electrons from sacrificial donor and quickly transfers to CoPyCl where proton reduction takes place. Thus, the PS of ZnDC(*p*-NI)PP porphyrin produced hydrogen evolution rate (ηH_2) of 35.70 mmol g^{-1} h^{-1}, which is 8-fold higher than the control porphyrin ZnDCPP which lacks the NI groups (4.64 mmol g^{-1} h^{-1}) and even 15-fold higher than typical porphyrin, ZnTCPP (2.43 mmol g^{-1} h^{-1}).

Results and discussion

Experimental Section

The synthetic protocol used for the preparation of ZnDC(*p*-NI)PP is shown in Scheme 1. The di-bromozinc derivative, DiBrZnD(*p*-NI)PP was synthesized by bromination of D(*p*-NI)PPH_2 with NBS reagent followed by reaction with $Zn(OAC)_2.2H_2O$. Subsequently, reaction of DiBrZnD(*p*-NI)PP with 4-carboxyphenyl boronic acid under Suzuki-Miyaura coupling reaction yielded target ZnDC(*p*-NI)PP porphyrin. The controlled porphyrin ZnDCPP was synthesized in two steps (Scheme S1). Firstly, the acid catalyzed condensation of phenyl dipyyrolomethane with 4-formylmethylbenzoate produced the DMMPPH2 porphyrin and zinc metalation of this gave ZnDMCPP. In the second step, demethylation of ZnDMCPP under basic conditions resulted in ZnDCPP porphyrin zinc(II)-

tetracarboxyphenylporphyrin (ZnTCPP) was synthesized for comparison (Scheme S2). Both porphyrins were thoroughly characterized by NMR and MALDI-TOF techniques.

Optoelectronic properties

The absorption and emission spectra of the porphyrins are shown in Fig. 2 and the corresponding data are noted in table 1. All the porphyrins mainly show two types of peaks. The broad and intensified peaks located at ca. 420-440 nm correspond to the Soret band absorption and the less intensified peaks positioned at ca. 500-650 nm are attributed to the Q-bands absorption. For ZnDC(*p*-NI)PP porphyrin, the additional peaks at higher energy region (ca. 350 nm) could be ascertained to the NI absorption peaks. Notably, ZnDC(*p*-NI)PP porphyrin shows apparently higher molar extinction coefficient (ε) values for Soret- and Q-bands than the ZnDCPP which lacks the NI groups and ZnTCPP featuring four carboxylic groups. This could be attributed to the conjugation of NI donor chromophores to the *meso*-positions of porphyrin acceptor which might affected the electronic transition probability between the $^1S_0$–^1E_u and $^1S_0$–^2E_u transitions of porphyrin macrocycle.[33] These results clearly speculate that conjugation of NI donor chromophores at *meso*-position of porphyrin moiety could enhance the light-harvesting ability in the UV-Visible region and consequently expectable good PHE results. It is noted ZnTCPP shows a lower ε value for Soret band than ZnDC(p-NI)PP and ZnDCPP.

All the porphyrins show two emission peaks in the region of 600-700 nm under excitation of 420 nm which belongs to Soret band of porphyrin moiety. The intensified emission peaks at ca. 610 nm and weak emitting peaks at ca. 660 nm correspond to the Q(0,0) and Q(1,0), respectively of porphyrin macrocycle. In our previous reports, we have already demonstrated the occurrence of intramolecular Förster resonance energy transfer (FRET) between NI donor chromophores and porphyrin acceptor due to the overlap emission spectrum of NI and absorption spectrum of porphyrin ring.[32-34] Accordingly, as ZnDC(*p*-NI)PP porphyrin bearing the NI there would be FRET between NI moieties and porphyrin ring. In general, NI chromophore shows very strong emission peak at ca. 450 nm under the excitation of 330 nm which corresponds to NI absorption. Impressively, the absence of NI emission peak in the ZnDC(*p*-NI)PP emission spectrum under the excitation of 330 nm clearly indicates the efficient FRET between the NI donor and the porphyrin acceptor. The calculated FRET efficiency (Φ_{ET}) of ZnDC(*p*-NI)PP is 99%. Since the fluorescence lifetime (t_F) of the porphyrin is directly related to the stability of porphyrin excited states, calculation of t_F could give more insight into the porphyrin photoexcited states (Fig. 3(a)). The order of calculated t_F of the porphyrins is as follows: ZnDC(*p*-NI)PP (3.8 ns) > ZnDCPP (2.4 ns) > ZnTCPP (1.8 ns). Among the three porphyrins, the ZnDC(*p*-NI)PP bearing the NI moieties showed the highest t_F. This obviously indicates that the ZnDC(*p*-NI)PP possesses highly stabilized photoexcited states. The higher t_F of ZnDC(*p*-NI)PP than the ZnDCPP and ZnTCPP could be ascribed to the efficient FRET between NI and porphyrin moieties. Moreover, the controlled porphyrin, ZnDCPP also shows higher t_F than the commonly used ZnTCPP. It indicates that the porphyrin with two carboxylic groups possesses long lived photoexcited states than the congener porphyrin with four COOH groups. The calculated photoluminescence quantum yield (Φ_F) of the porphyrins is in the order of ZnDC(*p*-NI)PP (18%) > ZnDCPP (13% ns) > ZnTCPP (10% ns) which is also in line to the their t_F trend.

The thermodynamic viability of electron transfer during the PHE cycle depends mainly on the excited state oxidation potentials ($E_{(P^+/P^*)}$) and excited state reduction potentials ($E_{(P^*/P^-)}$) of the porphyrins.[35] Since such relative energies can't be evaluated directly, firstly, we calculated the first oxidation potential (E_{Ox}) and first reduction potential (E_{Red}) values which correspond to HOMO and LUMO of the porphyrins, respectively, by performing the cyclic voltammetric

experiments in THF solution (Fig. S1). The calculated E_{Ox} values of ZnDC(*p*-NI)PP, ZnDCPP and ZnTCPP are 1.23, 1.22, and 1.20 V, respectively. And the values – 1.13, – 1.19, and – 0.83 V correspond to the E_{Red} of ZnDC(*p*-NI)PP, ZnDCPP and ZnTCPP, respectively. According to Rehm−Weller equations (see footnote in Table 1), the ($E_{(P^+/P^*)}$) values of the ZnDC(*p*-NI)PP, ZnDCPP and ZnTCPP were calculated to be – 0.94, – 0.97, and – 0.95 V, respectively and ($E_{(P^*/P^-)}$) values of the porphyrins ZnDC(*p*-NI)PP, ZnDCPP and ZnTCPP were calculated to be 1.04, 1.00, and 1.32 V, respectively. As seen in Fig. 3(b), the ($E_{(P^*/P^-)}$) values of the porphyrins are more positive than the oxidation potential (E_{ox}) of ascorbic acid (AA) sacrificial electron donor indicating a favourable thermodynamic driving force for electron transfer from AA to photoexcited porphyrins. And the ($E_{(P^+/P^*)}$) values of porphyrins are more negative than the reduction potential (E_{ox}) of CoPyCl cocatalyst suggesting an effective transfer of electrons from photoexcited porphyrin to CoPyCl where proton reduction takes place. The relatively high-lying ($E_{(P^*/P^-)}$) value of ZnDC(*p*-NI)PP than the ZnTCPP should be helpful for more efficient electron transfer from AA to photoexcited porphyrins and thus expectable higher PHE performance for ZnDC(*p*-NI)PP than that of ZnTCPP.

PHE studies

In order to evaluate the PHE properties of porphyrins, a series of homogeneous PSs were prepared in buffer/THF solution by employing porphyrins as photosensitizers, AA as sacrificial electron donor and CoPyCl as cocatalyst. The optimized PHE properties of PSs are shown in Fig. 4 and the corresponding data are noted in Table 2. Fig. 4 shows the hydrogen evolution rate (ηH_2) of the PSs under the illumination of OLED light source for 5 h. From Fig. 4(a), it was noticed that the ZnDC(*p*-NI)PP bearing the NI donor chromophores and -COOH groups displayed higher ηH_2 than the ZnDCPP which lacks the NI moieties and well known ZnTCPP. The ηH_2 order of PS of the porphyrins is ZnDC(*p*-NI)PP (35.70 mmol g^{-1} h^{-1}) > ZnDCPP (4.64 mmol g^{-1} h^{-1}) > ZnTCPP (2.43 mmol g^{-1} h^{-1}). The calculated apparent quantum yield (AQE) of ZnDC(*p*-NI)PP, ZnDCPP and ZnTCPP PSs are 10.01%, 1.30% and 1.00%, respectively. The AQE values of PSs also well match to their ηH_2 order. Furthermore, under the optimized conditions, the photostability of the three porphyrins PSs was also evaluated by measuring their PHE up to 50 h of light irradiation. As seen in Fig. 4(b), the PHE of the three porphyrins was gradually increased with time indicating the good photostability of all components. The appearance of similar absorption and emission spectra of PSs before and after light irradiation also attests to their good photostability under light irradiation (Fig. S11 & S12). The order of turnover number (TON) of the three PSs is as follows: ZnDC(*p*-NI)PP (5958), ZnDCPP (1397) and ZnTCPP (562) which is also in line to their ηH_2 and AQE trends. More importantly, the ηH_2 and TON of ZnDC(*p*-NI)PP PS is superior to the PSs comprising porphyrin photosensitizers and cobaloxime catalysts so far in the literature (Table S1).[30, 31, 36, 37] Particularly, the ηH_2 of ZnDC(*p*-NI)PP PS is 3.3 times higher than the most efficient PS containing water soluble porphyrin photosensitizer, PorFN (10.9 mmol g^{-1} h^{-1}) and Pt cocatalyst reported recently.[38] Moreover, the ηH_2 of ZnDC(*p*-NI)PP is also much higher than our recently reported iridium-conjugated porphyrins[39] and far better than the NI-conjugated porphyrins under heterogeneous conditions with Pt cocatalyst.[32-34] The superior PHE properties of ZnDC(*p*-NI)PP possessing the 5,15-di(NI) substituted porphyrin donor chromophores than the ZnDCPP which lacks the NI could be explained by the following factors; (i) good light-harvesting properties in the UV-vis region of solar spectrum, (ii) the efficient FRET from the NI donor to the porphyrin acceptor would stabilize the photoexcited states of porphyrin ring and thus long-lived photoexcited electron lifetime which further enhances the electron transfer from the photo-excited porphyrin moiety to the CoPyCl through COOH groups, (iii) An efficient acceptance of electrons from AA and subsequent transfer to CoPyCl (vide infra). Under the optimized PHE conditions of porphyrins, we also tested the ηH_2 of PSs of porphyrins using Pt cocatalyst (2 wt%) instead of CoPyCl cocatalyst (Fig. S3). The results indicate that the Pt cocatalyst-based PSs showed lower ηH_2 than the PSs of CoPyCl cocatalyst. Nevertheless, the PS of porphyrins were tested by varying the concentration of porphyrins (Fig. S4) and the nature

of sacrificial donors such as TEA (Fig. S5). All the experiments' output disclose that the PS conditions of Fig. 4 is the best to produce the efficient PHE.

To further understand the molecular design of ZnDC(*p*-NI)PP, we evaluated the ηH_2 of our recently published efficient ZnD(*p*-NI)PP which contains two NI moieties and lacks the COOH groups. The PS of ZnD(*p*-NI)PP exhibited ηH_2 of 3.8 mmol g^{-1} h^{-1} (Fig. S2, table 2), which is 10-fold lower than the PS of ZnDC(*p*-NI)PP. Similarly, the PHE of methylated ZnDCPP and ZnTCPP porphyrins such as ZnDMCPP and ZnTMCPP, respectively were also tested for better comparison. The ηH_2 of ZnDMCPP (1.2 mmol g^{-1} h^{-1}) and ZnTMCPP (0.9 mmol g^{-1} h^{-1}) is lower than their congener porphyrins, ZnDCPP and ZnTCPP possessing the COOH groups (Fig. S2). All these results clearly suggest that

there would be close contact between COOH of ZnDC(*p*-NI)PP and CoPyCl in the solution of PS. Nevertheless, the Soret band peak of ZnDC(*p*-NI)PP is gradually red-shifted and splitted with increasing the concertation of CoPyCl by titration, attributed to the electrostatic interactions between cationic Co(III) and negatively charged ZnDC(*p*-NI)PP molecules (Fig. S6).[38] Thus under light irradiation, the higher performance of ZnDC(*p*-NI)PP in PHE is attributed to the FRET from the NI donor chromophore to the porphyrin acceptor that would promote the long-lived photoexcitation states. At the same time, the anionic form ($-COO^-$) of 4-carboxyphenyl substituents at pH 7.4 enables a faster electron transfer from porphyrin to cationic Co(III) potentially due to electrostatic force.

In order to get more insight into the effect of CoPyCl and AA concentrations on ηH_2, we have prepared a series of PSs containing ZnDC(*p*-NI)PP and variable concentrations of CoPyCl and AA. From Fig. S7, it was observed that the concentration of both CoPyCl and AA has also played an important role to optimize the PSs. For achieving high ηH_2, the PSs must be prepared using 2.0 mM of CoPyCl and 0.4 M of AA. Since PHE of PSs is strongly dependent on pH, the PHE of ZnDC(*p*-NI)PP PS has been evaluated at different pH values. As seen in Fig. 5, the PS of ZnDC(*p*-NI)PP exhibited the highest ηH_2 of 35.70 mmol g^{-1} h^{-1} at pH = 7.4, under likely slightly basic condition. On the contrary, the PSs of ZnDC(*p*-NI)PP showed a gradual decrease in ηH_2 when pH either increased or decreased with respect to pH = 7.4. The declined PHE results of ZnDC(*p*-NI)PP PS under acidic conditions could be attributed to the degradation of AA which hampers the reducing nature of photoexcited photosensitizer, whereas the rate of formation of active cobalt hydride catalytic intermediate is low under basic conditions and consequently reduces proton reduction.[40]

Generally, the electron transfer mechanism involved in homogeneous PHE systems comprising photosensitizer, sacrificial donor and cocatalyst proceeds through either oxidative or reductive quenching pathways. The dominance of quenching type dictates the multistep electron transfer pathway in PSs. The oxidative quenching mechanism involves the transfer of photoexcited electrons of photosensitizer to cocatalyst followed by oxidized photosensitizer reduced back to original ground state by taking electrons from sacrificial donor. In the case of reductive quenching mechanism, the sacrificial donor reduces the excited photosensitizer which further returns to ground state by transferring electrons to cocatalyst where proton reduction takes place. Thus, to understand the type of electron transfer mechanism involved in our PSs, we have performed the quenching studies using CoPyCl and AA as quenchers (Fig. S8-S10). For instance, the fluorescence emission intensity of ZnDC(*p*-NI)PP is gradually decreased with increasing the concentration of either CoPyCl or AA (Fig. S4). It indicates that the photoexcited ZnDC(*p*-NI)PP could either efficiently accept an electron from AA or transfer electrons to CoPyCl. The calculated Stern-Volmer quenching constants (K_q) of ZnDC(*p*-NI)PP are 1.9×10^2 $M^{-1}s^{-1}$ and 4.2 $M^{-1}s^{-1}$ for quenchers CoPyCl and AA, respectively (Fig. 6). However, given the high concertation of AA (0.4 M) than the CoPyCl (2.0 mM) used in the PSs, the calculated oxidative and reductive quenching rates of ZnDC(*p*-NI)PP are 38×10^2 s^{-1} and 168×10^2 s^{-1}, respectively. Since the reductive quenching rate is 5 times higher than the oxidative quenching rate, the reductive quenching mechanism can be assigned to the current PSs. Accordingly, the calculated oxidative quenching rates of ZnDCPP and ZnTCPP are 1.6×10^{-2} and 4.6×10^{-2} s^{-1}, respectively whereas the values 0.57×10^{-4} and 0.15×10^{-4} s^{-1} correspond to the quenching rates of ZnDCPP and ZnTCPP, respectively. The reductive quenching rates order of porphyrins is ZnDC(*p*-NI)PP > ZnTCPP > ZnDCPP

whereas the order, ZnDC(*p*-NI)PP > ZnDCPP > ZnTCPP represents the oxidative quenching rates of the porphyrins. These quenching rates orders reveal that the ZnDC(*p*-NI)PP porphyrin can efficiently accept electrons from AA, which are further quickly donated to CoPyCl than the control porphyrins ZnDCPP and ZnTCPP. This result is also well consistent with higher PHE results for ZnDC(*p*-NI)PP PS than the PSs of ZnDCPP and ZnTCPP porphyrins.

Based on the optoelectronic, PHE and Stern-Volmer quenching studies, we have proposed a schematic illustration of electron transfer mechanism involved in the photo-redox cycle for hydrogen production (Fig. 7). Upon light irradiation on NI containing ZnDC(*p*-NI)PP porphyrin (denoted NI-P-COO^{-}), the photoexcited NI moiety transfers energy to porphyrin ring through IET process, followed by the formation of photoexcited porphyrin complex [NI-P-COO^{-}]*. This complex then accepts an electron from AA resulting in reduced [NI-P-COO^{-}]$^{-}$ species which further donates two electrons to Co(III)PyCl to give reduced Co(I)PyCl. Finally, the resulting Co(I) species ultimately reduces protons to hydrogen.

The photoinduced hole-electron pair generation and separation of porphyrins also has tremendous role to transfer electrons from the excited porphyrins to cocatalyst and thereby evolve H_2. Thus, additionally, we have performed the photocurrent response studies for the porphyrins. As seen in Fig. S12, the photocurrent response of the porphyrins is in the following order: ZnDC(*p*-NI)PP > ZnDCPP > ZnTCPP. Among all, ZnDC(*p*-NI)PP porphyrin displayed higher photocurrent response than the congener porphyrins ZnDCPP and ZnTCPP suggesting the efficient photoinduced hole-electron pair separation and migration of electrons for the former porphyrin. This result is also in line with the higher PHE of ZnDC(p-NI)PP than the ZnDCPP and ZnTCPP.

Conclusions

In summary, we designed and synthesized a new porphyrin ZnDC(*p*-NI)PP bearing two NI donor chromophores and two 4-carboxyphenyl substituents. Absorption and emission spectra explored that the introduction of two NI moieties onto *meso*-position of porphyrin moiety enhanced the light harvesting properties, t_F and Φ_F values. Stern-Volmer quenching studies suggested that the electron transfer rate from porphyrin center to CoPyCl was tremendously enhanced for ZnDC(*p*-NI)PP. This could be ascribed to the stabilized photoexcited states of ZnDC(*p*-NI)PP due to efficient energy transfer form NI moieties to porphyrin ring. In addition, the anionic form of the 4-carboxyphenyl substituents also facilitated the faster electron transfer between the porphyrin centre and cationic Co(III) due to electrostatic force. Photocurrent response studies also revealed that the ZnDC(*p*-NI)PP showed higher photoinduced charge carriers generation and separation than the ZnDCPP. As a consequence, the homogeneous PS of ZnDC(*p*-NI)PP produced higher PHE properties such as ηH_2 of 35.6 mmol g^{-1} h^{-1}, TON of 5958 and AQE of 10.01% than those of ZnDCPP PS (ηH_2 of 4.64 mmol g^{-1} h^{-1} TON of 1397 and AQE of 1.3%) and the typical ZnTCPP porphyrin bearing four COOH (ηH_2 of 2.43 mmol g^{-1} h^{-1} TON of 562 and AQE of 1.0%). Since ZnDC(*p*-NI)PP porphyrin produced very high PHE results, the studies of ZnDC(*p*-NI)PP and graphitic carbon nitride (g-C_3N_4) hybrid materials for H_2 evolution and CO_2 reduction are under investigation in our laboratory.

Conflicts of interest

There are no conflicts to declare.

Acknowledgements

The research was supported by General Research Fund (HKBU 12304320) from the Hong Kong Research Grants Council, and Initiation Grant for Faculty Niche Research Areas (IG-FNRA)

(2020/21)-RC-FNRA-IG/20-21/SCI/06 from Research Committee of Hong Kong Baptist University. W.-Y.W. thanks the financial support from the Science, Technology and Innovation Committee of Shenzhen Municipality (JCYJ20180507183413211), the RGC Senior Research Fellowship Scheme (SRFS2021-5S01), the Hong Kong Polytechnic University (1-ZE1C), Research Institute for Smart Energy (RISE) and Ms. Clarea Au for the Endowed Professorship in Energy (847S).

Notes and references

1. A. Fujishima and K. Honda, *Nature*, 1972, **238**, 37.
2. Y. Tachibana, L. Vayssieres and J. R. Durrant, *Nat. Photonics*, 2012, **6**, 511.
3. N. Armaroli and V. Balzani, *Angew. Chem., Int. Ed.,* 2007, **46**, 52-66.
4. B. Zhang and L. Sun, *Chem. Soc. Rev.*, 2019, **48**, 2216-2264.
5. M. Kirch, J.-M. Lehn and J.-P. Sauvage, *Helv. Chim. Acta*, 1979, **62**, 1345-1384.
6. I. N. Mills, J. A. Porras and S. Bernhard, *Acc. Chem. Res.*, 2018, **51**, 352-364.
7. X. Zhang, T. Peng and S. Song, *J. Mater. Chem. A*, 2016, **4**, 2365-2402.
8. O. J. Stacey and S. J. A. Pope, *RSC Adv.*, 2013, **3**, 25550-25564.
9. D. Li, J. Shi and C. Li, *Small*, 2018, **14**, 1704179.
10. Y. Shi, A.-F. Yang, C.-S. Cao and B. Zhao, *Coord. Chem. Rev.*, 2019, **390**, 50-75.
11. H. Wang, H. Wang, Z. Wang, L. Tang, G. Zeng, P. Xu, M. Chen, T. Xiong, C. Zhou, X. Li, D. Huang, Y. Zhu, Z. Wang and J. Tang, *Chem. Soc. Rev.,* 2020, **49**, 4135-4165.
12. T.-X. Wang, H.-P. Liang, D. A. Anito, X. Ding and B.-H. Han, *J. Mater. Chem. A,* 2020, **8**, 7003-7034.
13. J. Jayakumar and H.-H. Chou, *ChemCatChem.*, 2020, **12**, 689-704.
14. C. Xu, W. Zhang, J. Tang, C. Pan and G. Yu, *Front. Chem.*, 2018, **6**.
15. J. Wen, J. Xie, X. Chen and X. Li, *Appl. Surf. Sci.,* 2017, **391**, 72-123.
16. S. W. Cao, J. X. Low, J. G. Yu and M. Jaroniec, *Adv. Mater.*, 2015, **27**, 2150-2176.
17. S. Fukuzumi, Y.-M. Lee and W. Nam, *J Porphyr. Phthalocyanines.*, 2020, **24**, 21-32.
18. K. Ladomenou, M. Natali, E. Iengo, G. Charalampidis, F. Scandola and A. G. Coutsolelos, *Coord. Chem. Rev.*, 2015, **304-305**, 38-54.
19. X. Fang, Q. Shang, Y. Wang, L. Jiao, T. Yao, Y. Li, Q. Zhang, Y. Luo and H.-L. Jiang, *Adv. Mater*., 2018, **30**, 1705112.
20. Y. Qian, D. Li, Y. Han and H.-L. Jiang, *J. Am. Chem. Soc.*, 2020, **142**, 20763-20771.
21. P. Kumar, R. Boukherroub and K. Shankar, *J. Mater. Chem. A*, 2018, **6**, 12876-12931.
22. J. Yang, H. Yan, X. Zong, F. Wen, M. Liu and C. Li, *Philos. Trans. Royal Soc. A.*, 2013, **371**, 20110430.
23. C. Lentz, O. Schott, T. Auvray, G. S. Hanan and B. Elias, *Dalton Trans.,* 2019, **48**, 15567-15576.
24. F. Gärtner, S. Denurra, S. Losse, A. Neubauer, A. Boddien, A. Gopinathan, A. Spannenberg, H. Junge, S. Lochbrunner, M. Blug, S. Hoch, J. Busse, S. Gladiali and M. Beller, *Chem. Eur. J.,* 2012, **18**, 3220-3225.
25. D. Dolui, S. Khandelwal, P. Majumder and A. Dutta, *Chem. Commun.,* 2020, **56**, 8166-8181.
26. J.-W. Wang, W.-J. Liu, D.-C. Zhong and T.-B. Lu, *Coord. Chem. Rev.*, 2019, **378**, 237-261.
27. Z. Han, L. Shen, W. W. Brennessel, P. L. Holland and R. Eisenberg, *J. Am. Chem. Soc.*, 2013, **135**, 14659-14669.
28. P. Zhang, J. Hu, B. Liu, J. Yang and H. Hou, *Chemosphere*, 2019, **219**, 617-635.
29. A. Fihri, V. Artero, M. Razavet, C. Baffert, W. Leibl and M. Fontecave, *Angew. Chem., Int. Ed.,* 2008, **47**, 564-567.

30. P. Zhang, M. Wang, C. Li, X. Li, J. Dong and L. Sun, *Chem. Commun.,* 2010, **46**, 8806-8808.
31. T. Lazarides, M. Delor, I. V. Sazanovich, T. M. McCormick, I. Georgakaki, G. Charalambidis, J. A. Weinstein and A. G. Coutsolelos, *Chem. Commun.,* 2014, **50**, 521-523.
32. G. B. Bodedla, J. Huang, W.-Y. Wong and X. Zhu, *ACS Appl. Nano Mater.*, 2020, **3**, 7040-7046.
33. G. B. Bodedla, L. Li, Y. Che, Y. Jiang, J. Huang, J. Zhao and X. Zhu, *Chem. Commun.*, 2018, **54**, 11614-11617.
34. G. B. Bodedla, G. Tang, J. Zhao and X. Zhu, *Sustain. Energy Fuels*, 2020, **4**, 2675-2679.
35. G. B. Bodedla, D. N. Tritton, X. Chen, J. Zhao, Z. Guo, K. C.-F. Leung, W.-Y. Wong and X. Zhu, *ACS Appl. Energy Mater.,* 2021, **4**, 3945-3951.
36. N. Queyriaux, E. Giannoudis, C. D. Windle, S. Roy, J. Pécaut, A. G. Coutsolelos, V. Artero and M. Chavarot-Kerlidou, *Sustain. Energy Fuels*, 2018, **2**, 553-557.
37. E. Giannoudis, E. Benazzi, J. Karlsson, G. Copley, S. Panagiotakis, G. Landrou, P. Angaridis, V. Nikolaou, C. Matthaiaki, G. Charalambidis, E. A. Gibson and A. G. Coutsolelos, *Inorg. Chem.*, 2020, **59**, 1611-1621.
38. X. Yang, Z. Hu, Q. Yin, C. Shu, X.-F. Jiang, J. Zhang, X. Wang, J.-X. Jiang, F. Huang and Y. Cao, *Adv. Funct. Mater.*, 2019, **29**, 1808156.
39. D. N. Tritton, G. B. Bodedla, G. Tang, J. Zhao, C.-S. Kwan, K. C.-F. Leung, W.-Y. Wong and X. Zhu, *J. Mater. Chem. A*, 2020, **8**, 3005-3010.
40. B. B. Beyene and C.-H. Hung, *Sustain. Energy Fuels,* 2018, **2**, 2036-2043.

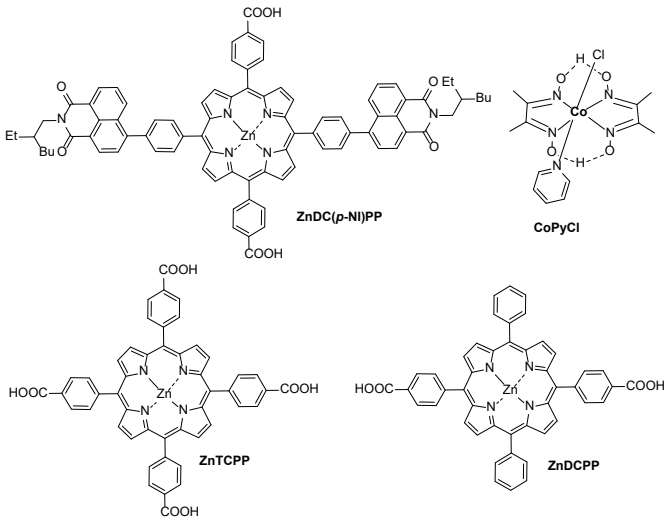

Fig. 1 Structures of the porphyrins used in this study.

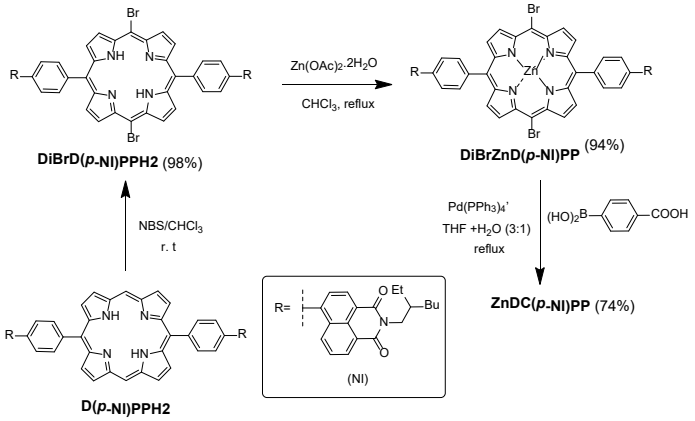

Scheme 1. Synthetic route for the preparation of ZnDC(p-NI))PP porphyrin.

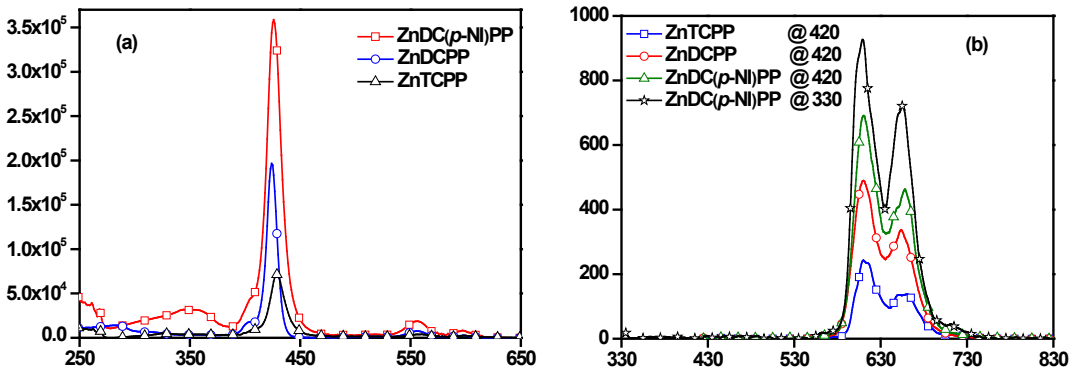

Fig. 2 (a) Absorption and (b) emission spectra of the dyes recorded in phosphate buffer/THF (9:1 v/v, 10 µM, pH = 7.4)) solution. All the porphyrins were excited at 420 nm and additionally, ZnDC(p-NI)PP was also excited at 330 nm to understand the intramolecular energy transfer between NI donor and porphyrin acceptor.

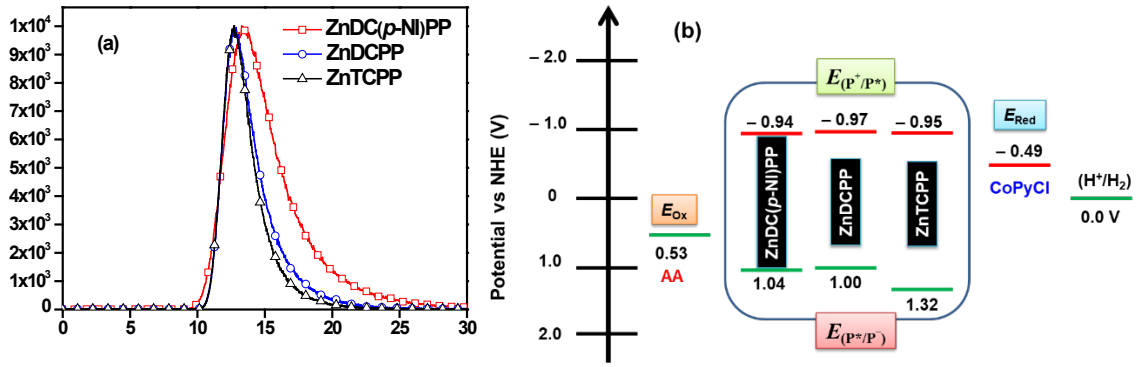

Fig. 3 (a) Lifetime decay spectra of the porphyrins recorded in in phosphate buffer/THF (9:1 v/v, 10 µM) solution at room temperature and (b) energy level alignment of the porphyrins, sacrificial donor and water reduction catalyst.

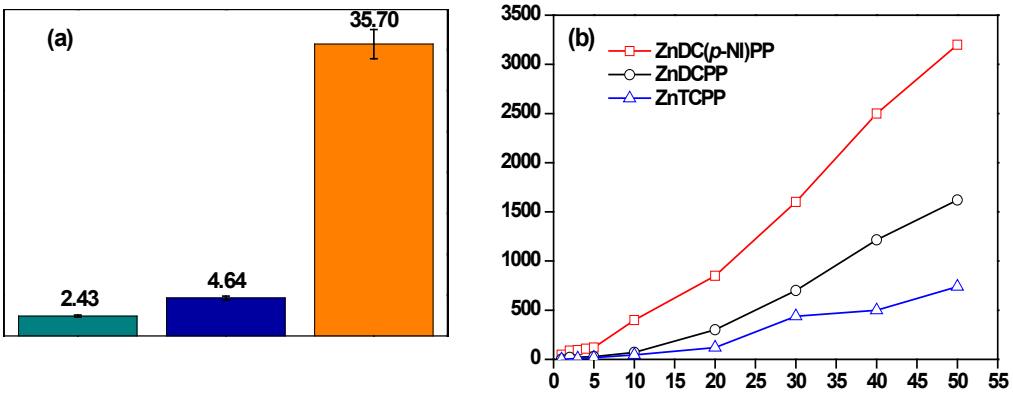

Fig. 4 (a) H_2 production rate of photocatalytic systems under the irradiation for 5 h and (b) H_2 production of photocatalytic systems under the irradiation (white LED light (148.5 mW/cm^2)) for 50 h: (Porphyrin (10 µM) + CoPyCl (2 mM) + AA (0.4 M) + buffer/THF (9:1 v/v) at pH 7.4)

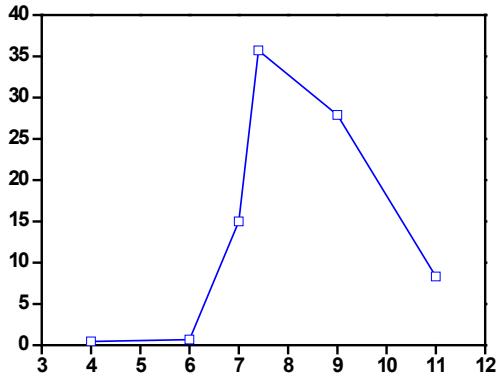

Fig. 5 H_2 production rate of photocatalytic systems at different pH under the irradiation for 5 h: (Porphyrin (10 μM) + CoPyCl (2.0 mM) + AA (0.4 M) + buffer/THF (9:1 v/v)).

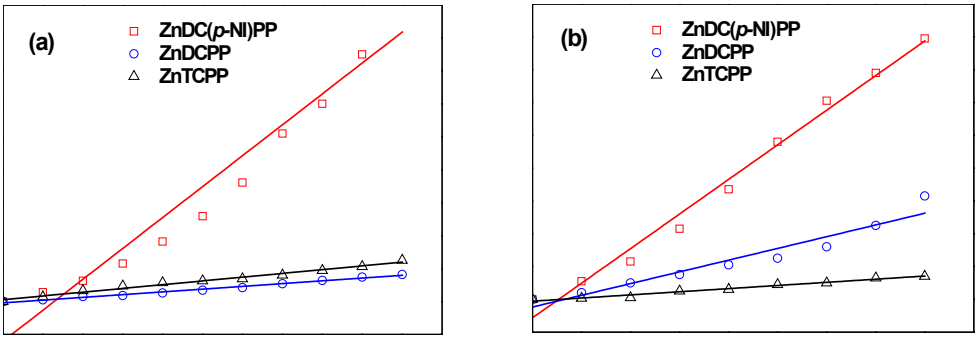

Fig. 6 Stern-Volmer plot of porphyrins (10 µM) with (a) CoPyCl and (b) AA as quencher in buffer/THF solution mixture.

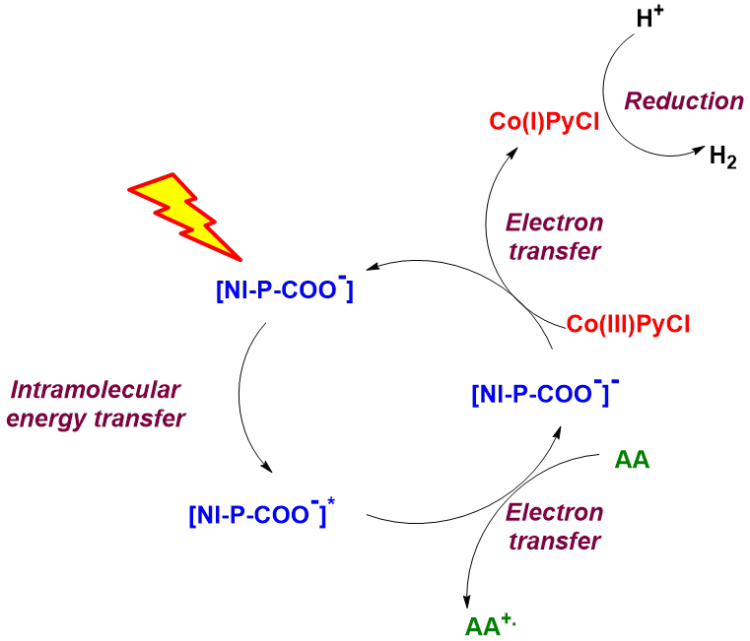

Fig. 7 Schematic illustration of photo-redox cycle mechanism for PHE with ZnDC(*p*-NI)PP, where NI-P-COO^- represents ZnDC(*p*-NI)PP.

Table 1. Optical properties of the dyes recorded in buffer/THF (9:1 v/v) solution

Porphyrin	λ_{abs}[a] (εx10^4, M^{-1} cm^{-1}) (nm)	λ_{em}[b] (nm)	Φ_F[c]	t_F[d] (nm)	E_{Ox}[e] (V)	E_{Red}[f] (V)	$E_{(P^+/P^*)}$[g] (V)	$E_{(P^*/P^-)}$[h] (V)	$E_{0\text{-}0}$[i]
ZnDC(*p*-NI)PP	350 (3.18), 426 (35.88), 556 (1.82), 597 (0.78)	611, 653	0.18	3.8	1.23, 1.53	– 1.13	– 0.94	1.04	2.17
ZnDCPP	424 (19.66), 556 (0.77), 599 (0.26)	609, 655	0.13	2.4	1.22, 1.54	– 1.19	– 0.97	1.00	2.19
ZnTCPP	429 (7.15), 560 (0.40), 599 (0.27)	610, 660	0.10	1.8	1.20, 1.48	– 0.83, – 1.17	– 0.95	1.32	2.15

[a,b,c,d] Phosphate buffer/THF (9:1 v/v) solution. [e] E_{ox} (vs NHE) = 0.77 + E_{ox} (vs Ferrocene). [f] E_{red} (vs NHE) = 0.77 – E_{red} (vs Ferrocene). [g] $E_{(P^+/P^*)}$ (vs NHE) = E_{Ox} – $E_{0\text{-}0}$; here "P" refers to porphyrin photosensitizer. [h] $E_{(P^*/PS^-)}$ (vs NHE) = E_{Red} + $E_{0\text{-}0}$. [i] Estimated from the intersection of the normalized absorption and emission spectra.

Table 2. Amount of H_2 (ηH_2) and turnover number (TON), turnover frequency (TOF), apparent quantum yield (AQE) for the photocatalytic systems.

Porphyrin	ηH_2 [a] (mmol g^{-1} h^{-1})	TON [b]	AQE% [c]
ZnTCPP	2.43	562	1.00
ZnDCPP	4.64	1397	1.30
ZnDC(*p*-NI)PP	35.70	5958	10.01
ZnD(*p*-NI)PP	3.8	590	1.5

[a] Calculated under irradiation for 5 h. [b] Calculated under irradiation for 50 h. [c] Calculated under irradiation for 1 h